# Assignment of haem ligands and detection of electronic absorption bands of molybdenum in the di-haem periplasmic nitrate reductase of *Paracoccus pantotrophus*

Clive S. Butler[a,1], Stuart J. Ferguson[b], Ben C. Berks[a], Andrew J. Thomson[a], Myles R. Cheesman[a], David J. Richardson[a,*]

[a] *Centre for Metalloprotein Spectroscopy and Biology, School of Biological and Chemical Sciences, University of East Anglia, Norwich NR4 7TJ, UK*
[b] *Department of Biochemistry, University of Oxford, South Parks Road, Oxford OX1 3QU, UK*

Received 26 March 2001; revised 1 May 2001; accepted 1 May 2001

First published online 13 June 2001

Edited by Gunnar von Heijne

**Abstract The periplasmic nitrate reductase (NAP) from *Paracoccus pantotrophus* is a soluble two-subunit enzyme (NapAB) that binds two *c*-type haems, a [4Fe–4S] cluster and a bis-molybdopterin guanine dinucleotide cofactor that catalyses the reduction of nitrate to nitrite. In the present work the NapAB complex has been studied by magneto-optical spectroscopy to probe co-ordination of both the NapB haems and the NapA active site Mo. The absorption spectrum of the NapAB complex is dominated by features from the NapB *c*-type cytochromes. Using a combination of electron paramagnetic resonance spectroscopy and magnetic circular dichroism it was demonstrated that both haems are low-spin with bis-histidine axial ligation. In addition, a window between 600 and 800 nm was identified in which weak absorption features that may arise from Mo could be detected. The low-temperature MCD spectrum shows oppositely signed bands in this region (peak 648 nm, trough 714 nm) which have been assigned to S-to-Mo(V) charge transfer transitions. © 2001 Published by Elsevier Science B.V. on behalf of the Federation of European Biochemical Societies.**

*Key words:* Magnetic circular dichroism spectroscopy; Electron paramagnetic resonance spectroscopy; Heme ligand; Molybdoenzyme

## 1. Introduction

Nitrate reductases catalyse the reduction of nitrate ($NO_3^-$) to nitrite ($NO_2^-$). Bacteria express three distinct nitrate reductases, two are associated with energy-conserving respiratory electron transport pathways and the third with nitrate assimilation [1]. One of the respiratory enzymes is membrane-anchored with an active site in the cytoplasm and the other is a water-soluble periplasmic enzyme [2]. The assimilatory enzymes are located in the cytoplasm [1]. Analysis of the amino acid sequences of many bacterial nitrate reductases suggests that they are all members of the sub-group of molybdoenzymes that bind the molybdopterin guanine dinucleotide (MGD) form of the molybdopterin cofactor [2]. The soluble periplasmic nitrate reductase (NAP) from *Paracoccus pantotrophus* (previously classified as *Thiosphaera pantotropha* [3] and *Paracoccus denitrificans* GB17 [4]) contains a 16 kDa di-haem *c*-type cytochrome subunit (NapB) and an 80 kDa catalytic subunit (NapA) that binds an N-terminal [4Fe–4S] cluster and the MGD cofactor [2,5–7]. A third component of the NAP system is NapC, a membrane-anchored tetra-haem *c*-type cytochrome that mediates electron flow between membrane quinols/quinones and the NapAB complex [8].

The crystal structure of monomeric NapA from *Desulfovibrio desulfuricans* has been reported recently [9] and has revealed the presence of two MGD moieties per polypeptide (bis-MGD). This is consistent with crystal structures of three other members of the MGD family, namely the soluble periplasmic dimethyl sulphoxide reductases (DMSOR) from *Rhodobacter capsulatus* and *Rhodobacter sphaeroides*, the soluble formate dehydrogenase H (FdhH) from *Escherichia coli*, and the periplasmic trimethylamine *N*-oxide reductase from *Shewanella massilia* [10–14]. We have undertaken a detailed study of the Mo centre of NAP from *P. pantotrophus* using electron paramagnetic resonance (EPR) and EXAFS spectroscopies in order to determine Mo co-ordination during nitrate reduction [15,16]. Our observations suggest that Mo(VI) is a di-oxo species co-ordinated by five sulphur ligands, four provided by the two pterins at 2.43 Å and one provided by a cysteine ligand at 2.82 Å. Upon reduction with dithionite the Mo centre becomes a mono-oxo Mo(IV) species co-ordinated by three sulphur ligands at 2.35 Å. We have suggested that the loss of sulphur co-ordination, presumably by the displacement of one of the pterins, may play an important role in catalysis by allowing substrate to bind or modulating the redox potential.

Optical spectroscopy has not been widely applied to the study of molybdoenzymes since the presence of additional chromophores (haems and the iron–sulphur cluster) obscure the weak molybdenum transitions. In the present paper we report the first study of a periplasmic nitrate reductase (NapAB complex) using magneto-optical spectroscopy to probe both the NapB haems and the active site Mo.

*Corresponding author. Fax: (44)-1603-592250.
E-mail: d.richardson@uea.ac.uk

[1] Present address: School of Biochemistry and Genetics, The Medical School, University of Newcastle, Newcastle upon Tyne NE2 4HH, UK.

*Abbreviations:* MGD, molybdopterin guanine dinucleotide; NAP, periplasmic nitrate reductase; DMSOR, dimethyl sulfoxide reductase; EPR, electron paramagnetic resonance; MCD, magnetic circular dichroism

0014-5793/01/$20.00 © 2001 Published by Elsevier Science B.V. on behalf of the Federation of European Biochemical Societies.
PII: S0014-5793(01)02577-7

## 2. Material and methods

*P. pantotrophus* M6 was grown anaerobically on nitrate and the NapAB complex was purified as described by Berks et al. [6]. Purified samples were prepared in 20 mM HEPES, pH 7.2 and concentrated to ~300 μM for EPR and magnetic circular dichroism (MCD) analysis. Samples for MCD were exchanged into $D_2O$ buffer containing 20 mM Na-HEPES, pH* 7.2. pH* is the apparent pH of the buffer in $D_2O$ measured with a standard glass pH electrode.

EPR spectroscopy was performed on an X-band ER200-D spectrometer (Bruker Spectrospin) interfaced to an ESP1600 computer and fitted with a liquid helium flow cryostat (ESR-9; Oxford Instruments). Haem EPR spectra were recorded at 10 K, ca. 9.64 GHz microwave frequency, 2 mW microwave power and 1.0 mT field modulation amplitude. Mo(V) EPR spectra were recorded at 60 K, ca. 9.64 GHz microwave frequency, 2 mW microwave power and 0.1 mT field modulation amplitude. Spin concentration of samples was determined from integrations of their EPR absorption spectra by comparison to those of a 2 mM $Cu^{II}$-EDTA standard as in earlier work [16]. Electronic absorption spectra were recorded on a Hitachi UV3000 spectrophotometer. MCD spectra were measured using a split-coil superconducting solenoid, Oxford Instruments type SM-4, capable of generating a maximum magnetic field of 5 T. Spectropolarimeters Jasco J-500D and J-730 were employed for the wavelength ranges 240–1000 and 800–2000 nm, respectively.

## 3. Results and discussion

The room-temperature absorption spectrum of the air-oxidised NapAB complex is dominated by the spectrum of the NapB *c*-type cytochrome spectrum with bands at 408 nm and 525 nm (Fig. 1A). Low-temperature MCD spectra of air-oxidised NapAB were dominated by intense absorption bands over the wavelength range 300–600 nm (Fig. 1B). These are characteristic of low-spin ferric haem, which in the Soret region (~400 nm) of the MCD spectrum gives rise to a temperature-dependent derivative-shaped band with a peak to trough intensity of approximately 32 000 $M^{-1}$ $cm^{-1}$ per haem at 4.2 K. The presence of low-spin ferric haem in the NapAB complex is also supported by the typical features and intensities of α,β-MCD bands at 550–600 nm. No features typical of high-spin ferric haem were apparent in the 600–650 nm region. The porphyrin → Fe(III) charge transfer transition for low-spin ferric haem occurs in the near-IR region of the spectrum (800–2500 nm). This band is readily observed by MCD spectroscopy, with the peak wavelength being an excellent indicator of the axial ligands to the haem iron [17]. The near-IR MCD spectrum for NapAB is characteristic of a low-spin haem porphyrin → Fe(III) charge transfer band and has a maximum peak at ~1480 nm (Fig. 1C). A band at this wavelength is in the range for haems with bis-His ligation. No intense absorbance band at ~1725 nm characteristic of His-Met ligation could be detected. It is recognised, however, that an absorbance band at 1480 nm is also characteristic of His-Lys co-ordination [17].

Inspection of a multiple sequence alignment of NapB reveals that the haem *c* binding motif CxxCH occurs twice in the sequence and two further His residues are also highly conserved at positions 79 and 114 (Fig. 2). The absence of highly conserved lysine residues suggests that both haems are bis-His-ligated. However, lysine residues are apparent in *P. pantotrophus* NapB and other NapB proteins (Fig. 2). It is dangerous to derive amino acid ligation solely from sequence analysis, as illustrated by studies on the cytochrome $cd_1$ nitrite reductases [18]. Consequently EPR spectroscopic evidence in support of the absence of a Lys ligand was sought. In the

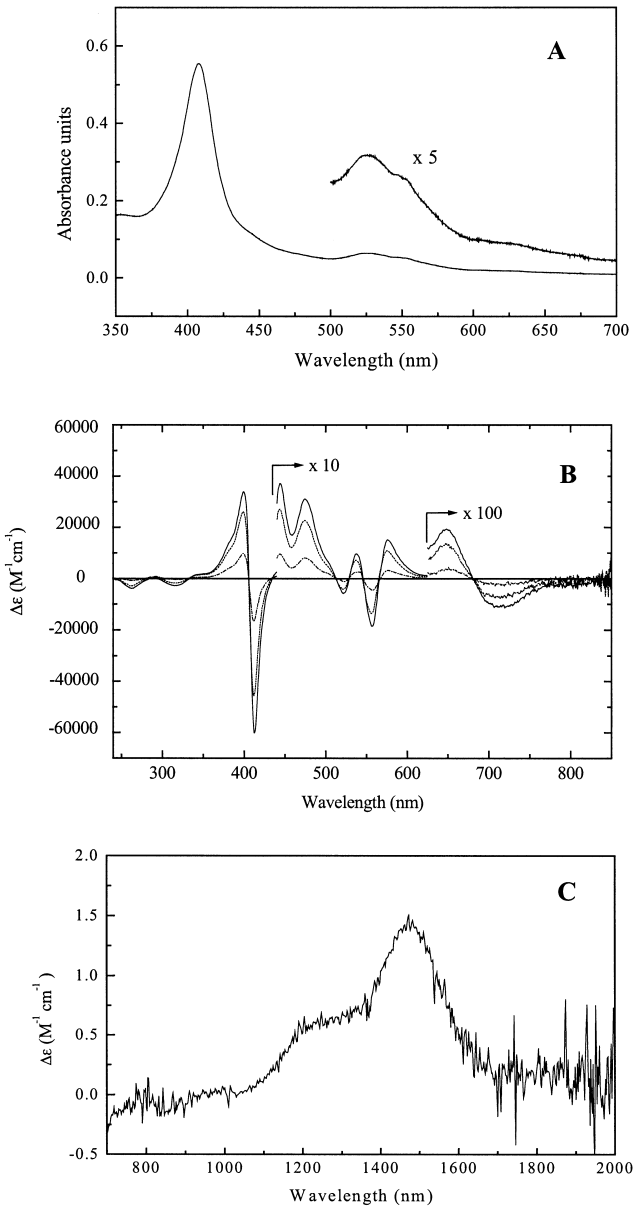


Fig. 1. Electronic absorption spectra of NapAB. A: Room-temperature absorption spectra of NapAB complex. B: Variable-temperature MCD spectra of the NapAB complex. Spectra were all collected at 5 T and recorded at 1.6 K (solid line), 4.2 K (dashed line) and 15.0 K (dot-dashed line). Enzyme was in 20 mM HEPES buffer, pH 7.2, diluted to 50% (v/v) with glycerol, at a final concentration of 293 μM. C: Room-temperature near-IR MCD spectrum of air-oxidised NapAB complex. Enzyme was in 20 mM HEPES $D_2O$ buffer, pH* 7.2, at a final concentration of 293 μM.

EPR spectra recorded at 10 K a rhombic signal with *g*-values 2.9, 2.2 and a broad feature at 1.5 could be detected which is typical of a low-spin ferric haem ($S = 1/2$) with two His ligands in which the imidazole planes are close to parallel (Fig. 3). Spin integration of the signal compared to a $Cu^{II}$ standard revealed ~1.7 mol of spin/mol of NAP, thus predicting that both haems in NapAB complex contributed to this signal. In addition, signals at $g \approx 2.01$, $g \approx 5.9$ and $g \approx 4.3$ were detected. These arise from an oxidised [3Fe–4S] cluster (~0.1 mol of spin/mol of NapAB; a product of the degradation of a small amount of [4Fe–4S] cluster during

```
        1                                                  50

Hinapb  ~~~~~VINMT KQVSKILAGL FTALFA.GSL MASDAPAVGK DLTQAAE..N
Ecnapb  MEFGSEIMKS HDLKKALC.Q WTAMLA.LVV SGAVWAANGV DFSQSPEVSG
Psnapb  ~~~MRSQDPS RRLSRRLWTL FALALC.LVT GTVALA.... Q..TVPQLSG
Rsnapb  ~~~~MSMHPA LRL......L ATVLVA.LGA GP.AFT.... Q..DAPRLTG
Ppnapb  ~~~MRGQDPS .RLIRPAAMA GLLLFA.LVG AALPQAEPAV Q..IVPALDR
Aenapb  ~~~~~~MKPS RSWASLLAVC AVLLAA.LAM QAIFFPAPAR AQGLVDAMRG
Cjnapb  ~~~~~~~~~~ ~MMKKKLVLL GSAAVVFFAA CAMNSGVSSE QIGLRKASLE

        51                                                 100
                                      *    **  **             *
Hinapb  IPPAFHN..A P......RQG ELPALNYVNQ PPMVPHSVAN .YQVTKNVNQ
Ecnapb  TQEGAIR..M P......KEQ DRMPLNYVNQ PPMIPHSVEG .YQVTTNTNR
Psnapb  RPSPMQNTGA DPLPRWIVDD IQKMRNYPDQ PPVIPHSIEG .YQLSVNTNR
Rsnapb  ADRPMSEVAA PPLPETITDD RRVGRNYPEQ PPVIPHAIEG .YQLSVNANR
Ppnapb  LGRADVRGQI PPLGRPITDD VRRMRNYPEQ PPVIPHSIDG .YQLTVNTNR
Aenapb  PTAIANEPRA PLLYPTENKD IRRTRNYTMQ PPTIPHKIDG .YQLDKDFNR
Cjnapb  NENKVNLVEA NFTTLQPGES TRFERSYENA PPLIPHAIED LLPITKDNNM

        101                                                150
        *  **                  *                   *   *  *** *
Hinapb  CLNCHSPENS RLSGATRISP THFMD.RDGK VGSS.SSPRR YFCLQCHVSQ
Ecnapb  CLQCHGVESY RTTGAPRISP THFMD.SDGK VGAE.VAPRR YFCLQCHVPQ
Psnapb  CMSCHRRELT EGSGAPMISV THYMN.REGQ MLAD.VSPRR YFCTACHVPQ
Rsnapb  CLECHRRQYS GLVAAPMISI THFQD.REGQ MLAD.VSPRR YFCTACHVPQ
Ppnapb  CMDCHKPQFT EGSGAPMISV THFQD.RDGQ VLTD.VTPRR YFCTACHVQQ
Aenapb  CMFCHARTRT EETQAIPVSI THYMD.RDNN VLAD.VSPRR YFCTQCHVPQ
Cjnapb  CLSCHDKAIA ADAGATPLPA SHYYDFRHNK TTGDMISDSR FNCTQCHVPQ

        151                                  186
                *  *
Hinapb  ANVDPIVPND FKPMKGYGN* ~~~~~~~~~~ ~~~~~~
Ecnapb  ADTAPIVGNT FTPSKGYGK* ~~~~~~~~~~ ~~~~~~
Psnapb  ADTRPLVDNT FKDMSE.LGF KPAGSGQ*~~ ~~~~~~
Rsnapb  TNAQPLVTNE FRDM...LTL TPASNEAE*~ ~~~~~~
Ppnapb  TDVQPLVPNQ FRDGYR.HAG GP*~~~~~~~ ~~~~~~
Aenapb  ADTKPLIGNN FVDVDTILKR RPGAKGAAK* ~~~~~~
Cjnapb  SDAKPLVGNS FKPEFKNEQL KSRSNLIDVI NEGVK*
```

Fig. 2. Multiple alignment of NapB sequences showing conserved histidine residues. Hi, *Haemophilus influenzae*; Ec, *Escherichia coli*; Ps, *Pseudomonas stutzeri*; Rs, *Rhodobacter sphaeroides*; Pp, *Paracoccus pantotrophus*; Ae, *Alcaligenes eutrophus*; Cj, *Campylobacter jejuni*.

purification), small levels of high-spin ferric haem (estimated $<1\%$ total haem) and adventitious ferric iron, respectively. His-Lys haem ligation is characterised by the presence of an EPR signal with $g_z \approx 3.5$ [17]. There was no evidence at any temperature (5–60 K) or power (1–200 mW) for such signal. The absence of a signal at $g \approx 3$–3.5 also suggests the absence of a haem with a 'large $g$ max' spectrum that would have been characteristic of a His-His ligated haem in which the imidazole planes are near-perpendicular rather than near-parallel.

A significant derivative feature with oppositely signed bands was detectable in the 4 K MCD spectrum between 600 and 800 nm, with $\Delta\varepsilon \approx 300$ $M^{-1}$ $cm^{-1}$ (Fig. 1B). The oxidised $[4Fe\text{–}4S]^{2+}$ cluster ($S=0$) in NapA is not expected to have transitions in this region. Given that the feature was detectable at low temperature ($\sim$1.6 K) and exhibited a temperature-dependent intensity (Fig. 1B), the transitions are most likely to arise from the paramagnetic Mo(V). Accordingly, EPR characterisation of the air-oxidised sample at 60 K confirmed the presence of the so-called high-$g$ [resting] Mo(V) species ($g_1 \approx 1.998$, $g_2 \approx 1.990$, $g_3 \approx 1.980$ and $g_{av} \approx 1.99$) [15,16], which accounted for around 10% of the total Mo. Similar oppositely signed MCD features have been reported for the Mo(V) species of the DMSOR from *R. capsulatus* [19] and *R. sphaeroides* [20]. The crystal structures of DMSOR from both *R. capsulatus* [11,12] and *R. sphaeroides* [10] have revealed that the Mo is co-ordinated by four sulphur ligands provided by two pterins and an oxygen ligand provided by a serine residue. The MCD transitions between 500 and 700 nm have been assigned to π-dithiolene-to-Mo(V) charge transfer transitions, with the two oppositely signed transitions assigned as $x$- and $z$-polarised charge transfer transitions, $2b_2(\pi) \rightarrow 3a_2(d_{xy})$ and $1a_2(\pi) \rightarrow 3a_2(d_{xy})$, respectively [20]. Sequence alignments and EXAFS analysis of *P. pantotrophus* NAP suggest, however, that the Mo is co-ordinated by a fifth sulphur ligand provided by a cysteine residue, replacing the Ser-O ligand in the DMSOR. Thus, the MCD features in the region 600–800 nm may arise from a combination of low-energy π-dithiolene-to-Mo(V) and thiolate-to-Mo(V) charge transfer transitions. It was not possible to detect higher-energy transitions from other Mo ligands such as oxo groups as features below 600 nm were obscured by signals from the NapB haems.

In conclusion, the present paper reports the first MCD study of a bacterial periplasmic nitrate reductase. The combination of MCD, EPR and amino acid sequence analysis suggests that the two haems of the NapB subunit are each low-spin $S=1/2$ species with bis-histidine haem coordination, in which the two imidazole rings have near-parallel planes. Sequence analysis places NapB in a distinct group from other multi-haem proteins and this represents the first information about haem iron ligation in this family. The intense haem absorbance bands mask some of the expected electronic transitions from other NapA cofactors. However, we have identified a window between 600 and 800 nm in which optical bands that we ascribe to the Mo cofactor can be detected. These absorption bands, although similar to those reported for DMSOR, are shifted to lower energy and may arise from either π-dithiolene-to-Mo(V) or thiolate-to-Mo(V) charge transfer transitions. Since the intensity and position of these transitions will be dependent upon the number and nature of the dithiolene and thiolate ligands to the molybdenum, variable-temperature magnetic circular dichroism (VTMCD) provides a valuable probe for sulphur co-ordination. We have reported previously a series of Mo(V) derivatives, namely low-$g$, high-$g$ [resting] [15] and high-$g$ [thiocyanate] [21] which may differ in their Mo–S co-ordination number and the ap-

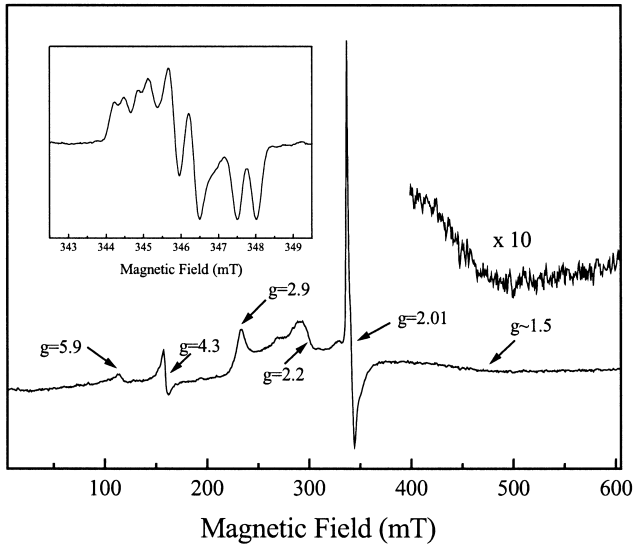


Fig. 3. X-band EPR spectrum of the NapAB complex. Conditions of measurement were: microwave frequency, 9.64 GHz; microwave power, 2 mW; modulation amplitude, 1.0 mT; temperature, 10 K. Inset shows the Mo(V) high-$g$ [resting] EPR signal. Conditions of measurement were: microwave frequency, 9.64 GHz; microwave power, 2 mW; modulation amplitude, 0.1 mT; temperature, 60 K.

plication of VTMCD will prove useful for characterising these species further.

*Acknowledgements:* This work was supported by BBSRC Grants GrCO8666 to D.J.R., B.C.B., A.J.T. and S.J.F., and BO3032-1 to the Centre for Metalloprotein Spectroscopy and Biology, University of East Anglia. We are grateful to Mr David Clarke, Mr Jeremy Thornton and Mrs Ann Reilly for help with the growth of *P. pantotrophus* and the purification of NAP.

## References

[1] Sears, H.J., Little, P.J., Richardson, D.J., Spiro, S., Berks, B.C. and Ferguson, S.J. (1997) Arch. Microbiol. 167, 61–66.
[2] Berks, B.C., Ferguson, S.J., Moir, J.W.B. and Richardson, D.J. (1995) Biochim. Biophys. Acta 1232, 97–173.
[3] Ludwig, W., Mittenhuber, G. and Freidrich, C.G. (1993) Int. J. Syst. Bacteriol. 43, 363–367.
[4] Rainey, F.A., Kelly, D.P., Stackebrandt, E., Burghardt, J., Hiraishi, A., Katayama, Y. and Wood, A.P. (1999) Int. J. Syst. Bacteriol. 49, 645–651.
[5] Berks, B.C., Richardson, D.J., Reilly, A., Willis, A.C. and Ferguson, S.J. (1995) Biochem. J. 309, 983–992.
[6] Berks, B.C., Richardson, D.J., Robinson, C., Reilly, A., Aplin, R.T. and Ferguson, S.J. (1994) Eur. J. Biochem. 220, 117–124.
[7] Breton, J., Berks, B.C., Reilly, A., Thomson, A.J., Ferguson, S.J. and Richardson, D.J. (1994) FEBS Lett. 345, 76–80.
[8] Roldan, M.D., Sears, H.J., Cheesman, M.R., Ferguson, S.J., Thomson, A.J., Berks, B.C. and Richardson, D.J. (1998) J. Biol. Chem. 273, 28785–28790.
[9] Dias, J.M., Than, M.E., Humm, A., Huber, R., Bourenkov, G.P., Bartunik, H.D., Bursakov, S., Calvete, J., Caldeira, J., Carneiro, C., Moura, J.J.G., Moura, I. and Romão, M.J. (1999) Structure 7, 65–79.
[10] Schindelin, H., Kisker, C., Hilton, J., Rajagopalan, K.V. and Rees, D.C. (1996) Science 272, 1615–1621.
[11] Schneider, F., Löwe, J., Huber, R., Schindelin, H. and Kisker, C. (1996) J. Mol. Biol. 263, 53–69.
[12] McAlpine, A.S., McEwan, A.G., Shaw, A.L. and Bailey, S. (1997) J. Biol. Inorg. Chem. 2, 690–701.
[13] Boyington, J.C., Gladyshev, V.N., Khangulov, S.V., Stadtman, T.C. and Sun, P.D. (1997) Science 275, 1305–1308.
[14] Czjzek, M., Dos Santos, J.P., Pommier, J., Giordano, G., Méjean, V. and Haser, R. (1998) J. Mol. Biol. 284, 435–447.
[15] Butler, C.S., Charnock, J.M., Bennett, B., Sears, H.J., Reilly, A.J., Ferguson, S.J., Garner, C.D., Lowe, D.J., Thomson, A.J., Berks, B.C. and Richardson, D.J. (1999) Biochemistry 38, 9000–9012.
[16] Bennett, B., Berks, B.C., Ferguson, S.J., Thomson, A.J. and Richardson, D.J. (1994) Eur. J. Biochem. 226, 789–798.
[17] Gadsby, P.M.A. and Thomson, A.J. (1990) J. Am. Chem. Soc. 112, 5003–5011.
[18] Allen, J.W.A., Watmough, N.J. and Ferguson, S.J. (2000) Nature Struct. Biol. 7, 885–888.
[19] Benson, N., Farrar, J.A., McEwan, A.G. and Thomson, A.J. (1992) FEBS Lett. 307, 169–172.
[20] Finnegan, M.G., Hilton, J., Rajagopalan, K.V. and Johnson, M.K. (1993) Inorg. Chem. 32, 2616–2617.
[21] Butler, C.S., Charnock, J.M., Garner, C.D., Thomson, A.J., Ferguson, S.J., Berks, B.C. and Richardson, D.J. (2000) Biochem. J. 352, 859–864.